Frontiers of Structural and Civil Engineering CN 10-1023/X
https://doi.org/10.1007/s11709-021-0706-z ISSN 2095-2430
RESEARCH ARTICLE

Analysis of stiffness and flexural strength of a reinforced concrete beam using an invented reinforcement system

Nazim Abdul NARIMAN[a]*, Martin HUSEK[b], Ilham Ibrahim MOHAMMAD[a], Kaywan Othman AHMED[a], Diyako DILSHAD[a], Ibrahim KHIDR[a]

[a]*Department of Civil Engineering, Tishk International University, Sulaimani 46001, Iraq*

[b]*Institute of Structural Mechanics, Faculty of Civil Engineering, Brno University of Technology, Brno 331/95-60200, Czech Republic*

**Corresponding author. E-mail: nazim.abdul@tiu.edu.iq*

Front. Struct. Civ. Eng., **Just Accepted Manuscript** • https://doi.org/10.1007/s11709-021-0706-z
http://journal.hep.com.cn on Mar 15, 2021

Article history: Received Mar 8, 2019; accepted May 8, 2020

Front. Struct. Civ. Eng. 2021
RESEARCH ARTICLE
https://doi.org/10.1007/s11709-021-0706-z

Analysis of stiffness and flexural strength of a reinforced concrete beam using an invented reinforcement system

Nazim Abdul NARIMAN[a]*, Martin HUSEK[b], Ilham Ibrahim MOHAMMAD[a], Kaywan Othman AHMED[a], Diyako DILSHAD[a], Ibrahim KHIDR[a]

[a]Department of Civil Engineering, Tishk International University, Sulaimani 46001, Iraq

[b]Institute of Structural Mechanics, Faculty of Civil Engineering, Brno University of Technology,

Brno 331/95-60200, Czech Republic

*Corresponding author. E-mail: nazim.abdul@tiu.edu.iq

ABSTRACT In this study, we conducted experimental tests on two specimens of reinforced concrete beams using a three-point bending test to optimize the flexure and stiffness designs. The first specimen is a reinforced concrete beam with an ordinary reinforcement, and the second specimen has an invented reinforcement system that consists of an ordinary reinforcement in addition to three additional bracings using steel bars and steel plates. The results of the flexure test were collected and analyzed, and the flexural strength, the rate of damage during bending, and the stiffness were determined. Finite element modeling was applied for both specimens using the LS-DYNA program, and the simulation results of the flexure test for the same outputs were determined. The results of the experimental tests showed that the flexural strength of the invented reinforcement system was significantly enhanced by 15.5% compared to the ordinary system. Moreover, the flexural cracks decreased to a significant extent, manifesting extremely small and narrow cracks in the flexure spread along the bottom face of the concrete. In addition, the maximum deflection for the invented reinforced concrete beam decreased to 1/3 compared to that of an ordinary reinforced concrete beam. The results were verified through numerical simulations, which demonstrated excellent similarities between the flexural failure and the stiffness of the beam. The invented reinforcement system exhibited a high capability in boosting the flexure design and stiffness.

KEYWORDS three-point flexure test, softening stage, flexural crack, flexural strain

1 Introduction

Plain concrete, which consists of aggregate, water, and cement, is weak in tension owing to the existence of numerous extremely small cracks in the structure of the concrete material. Under constant applied loading, these microcracks propagate in the concrete matrix [1]. Many types of moments and stresses, such as bending, shear, and torsion, are produced in the concrete structure owing to different loading application conditions. The stresses and moments, as well as the material flaws, human errors, and environmental situations become the source of degradation in concrete structures. When the concrete structures are damaged, they can either be destroyed, reconstructed, restored, or strengthened. Numerous studies have been conducted to find ways to overcome the deficiencies of normal concrete members, particularly in substantially loaded situations and parts susceptible to corrosion, such that a better strengthening mechanism can be applied [2,3].

Fracture mechanics is a branch or field of mechanics that is involved in the crack growth in any material during load application in all directions, and concerns cracks, stress areas near cracks, stress intensity factors within cracks, cracks resulting in failures, and crack growth. Excess tensile stress in a brittle fracture material causes cracks to be greater than the tensile strength. Crack development is rapid in solid materials such as plain concrete if the exerted load is greater than the toughness and resistance against fracture. As a result, a failure of the structural members or the entire structural system occurs.

Many techniques have been used by researchers to boost the flexural strength and stiffness of reinforced concrete structural members. In addition, many research studies have been conducted using invented techniques developed for the reinforcement system in concrete beams. In this study, a different reinforcement system was created, which comprises two additional strata of diagonal

RESEARCH ARTICLE
https://doi.org/10.1007/s11709-021-0706-z

bracing steel bars on the left and right sides of the beam connected to the longitudinal and stirrup reinforcements by welding, one strata of a bracing steel bar in the middle part along the beam, and the positioning of steel plates in both the compression and tension zones connected to the stirrups and longitudinal reinforcements through welding. This will add additional stiffness to the structural member by transferring the propagated stresses owing to load application at the center of the beam from the top compression zone to the bottom tension zone to restrict the tension and compression of the concrete fibers in both zones and automatically limit the plastic cracks and the deflection in the beam. We are studying the effects of an invented reinforcement system (which depends on the auto stabilization of the structural member under the applied bending load) for a concrete beam on the stiffness and flexural strength. We conducted two experiments using a three-point bending test for two specimens (an ordinary reinforcement system and an invented reinforcement system). Furthermore, a finite element analysis using the LS-DYNA program is being conducted for both models to verify the stiffness and flexural strength of the newly invented reinforcement system. The outputs of the present study can be adopted to search for the possibility of enhancing the performance of other structural elements such as reinforced concrete columns in withstanding lateral forces induced from earthquakes where the stiffness and shear strength can be assessed both experimentally and numerically.

2. Literature review

Many numerical methods have been used [4–8] to analyze fractures in concrete and reinforced concrete structures such as the partition of unity method, a particle method, mesh-free methods, and a cohesive crack method. The results of these studies have contributed to new approaches for understanding the behavior of concrete and steel materials under a fracture state.

Shishegaran et al. [9] suggested a new method for increasing the flexural capacity of reinforced concrete beams in a simply supported form. They used a new reinforcement steel bar layout that is bent up and covered with tubes made of rubber. They adopted a laboratory approach along with numerical modeling, and the results revealed an increase in the load-bearing capacity and stiffness of the structural elements. In addition, they formulated an equation to calculate the flexural capacity for the newly proposed reinforcement layout.

Mohammad and Aydin [10] proposed a reinforcement technique using a beam to enhance the flexural capacity that supports a closed rubber tube with a diameter equal to twice that of the reinforcement bar and covering the slanted part to separate it from the concrete of the beam. Consequently, they determined a 25% growth in the beam flexural capacity.

Researchers have worked on simulating the loading of plain concrete using the ABAQUS program. Namdar et al. [11] concluded that enhancing the physical properties of the concrete will increase the shear and flexural strengths of the beam.

In addition, an experimental method was implemented to estimate the stress distribution for a cracked reinforced concrete beam. Masmoudi et al. [12] discovered that the failure mode of beams reinforced with GFRP is slightly different from that of a normal beam. However, beams reinforced with GFRP fail either by concrete crushing of a concrete material at the compression zone or by a GFRP rupture.

Studies have incorporated steel fibers at different percentages to evaluate the response of the concrete beams to flexure and shear. Lana et al. [13] evaluated four beams, the first beam without steel fibers, and the remaining three beams reinforced with steel fibers at 0.5%, 0.8%, and 1.0%. The results displayed an important increase in the ductility and stiffness of steel-fiber reinforced beams. Consequently, changes in the mode of failure were monitored.

Steel plates have been used for strengthening purposes along the shear span of the beams. Sudarsana et al. [14] presented the results of the tests on the behavior of strengthened RC beams using steel plates fixed with bolts. The outputs indicated that the application of steel plates and bolts for external reinforcement enhance the shear capacity of the beam and the stiffness, and retarded the appearance of the diagonal cracks. Beams strengthened with plates in a U shape produce better executions compared to beams strengthened with two parts of L-shaped steel plates because of greater anchorages.

RESEARCH ARTICLE
https://doi.org/10.1007/s11709-021-0706-z

3 Flexural crack

A flexural crack appeared at the center of the beam span, which began at the bottom face of the beam and propagated to the top face. Theoretically, plain concrete is considered an isotropic material that behaves the same in all directions when subjected to an external load. To calculate both the stress **(**$\boldsymbol{\sigma}$**)** and strain **(**$\boldsymbol{\varepsilon}$**)** in such an isotropic material that behaves linearly elastically, the following three-dimensional case can be displayed [15]:

$$[\boldsymbol{\sigma}]=\begin{bmatrix}\sigma_x\\ \sigma_y\\ \sigma_z\\ \tau_{xy}\\ \tau_{yz}\\ \tau_{zx}\end{bmatrix},\ [\boldsymbol{\varepsilon}]=\begin{bmatrix}\varepsilon_x\\ \varepsilon_y\\ \varepsilon_z\\ \tau_{xy}\\ \tau_{yz}\\ \tau_{zx}\end{bmatrix}, \quad (1)$$

where $[\boldsymbol{\sigma}]=[\boldsymbol{C}][\boldsymbol{\varepsilon}]$ in which $[\boldsymbol{C}]$ is the elastic moduli matrix. Then,

$$[\boldsymbol{C}]=\frac{E}{(1+v)(1-v)}\begin{bmatrix}1-v & v & v & 0 & 0 & 0\\ v & 1-v & v & 0 & 0 & 0\\ v & v & 1-v & 0 & 0 & 0\\ 0 & 0 & 0 & \frac{(1-2v)}{2} & 0 & 0\\ 0 & 0 & 0 & 0 & \frac{(1-2v)}{2} & 0\\ 0 & 0 & 0 & 0 & 0 & \frac{(1-2v)}{2}\end{bmatrix}. \quad (2)$$

Both v and E can be substituted by K and G Consequently, $[\boldsymbol{C}]$ becomes

$$[\boldsymbol{C}]=\begin{bmatrix}K+\frac{4}{3}G & K-\frac{2}{3}G & k-\frac{2}{3}G & 0 & 0 & 0\\ K-\frac{2}{3}G & K+\frac{4}{3}G & K-\frac{2}{3}G & 0 & 0 & 0\\ K-\frac{2}{3}G & K-\frac{2}{3}G & K+\frac{4}{3}G & 0 & 0 & 0\\ 0 & 0 & 0 & G & 0 & 0\\ 0 & 0 & 0 & 0 & G & 0\\ 0 & 0 & 0 & 0 & 0 & G\end{bmatrix}. \quad (3)$$

By writing the equation in another form,

$$[\boldsymbol{\varepsilon}]=[\boldsymbol{C}]^{-1}[\boldsymbol{\sigma}]=[\boldsymbol{D}][\boldsymbol{\sigma}], \quad (4)$$

where $[\boldsymbol{D}]$ represents the inverse of $[\boldsymbol{C}]$.

RESEARCH ARTICLE
https://doi.org/10.1007/s11709-021-0706-z

$$[\boldsymbol{D}]=\frac{1}{E}\begin{bmatrix} 1 & -v & -v & 0 & 0 & 0 \\ -v & 1 & -v & 0 & 0 & 0 \\ -v & -v & 1 & 0 & 0 & 0 \\ 0 & 0 & 0 & \frac{1+v}{2} & 0 & 0 \\ 0 & 0 & 0 & 0 & \frac{1+v}{2} & 0 \\ 0 & 0 & 0 & 0 & 0 & \frac{1+v}{2} \end{bmatrix}. \quad (5)$$

The strain energy density $\boldsymbol{W}$, which is needed to deform the material, is as follows:

$$W=\int_0^{\varepsilon}\sigma \mathrm{d}\varepsilon. \quad (6)$$

The equation above represents the elastic behavior until the yield strain [16].

3.1 Flexural failure

In the long beams, flexural cracks appear owing to the effect of the maximum bending moment along the beam (Fig. 1). The failure is due to either an undue yielding of the longitudinal reinforcement, chased by the crushing of the concrete in the compression zone, resulting in a ductile failure under the beam or due to crushing of the compression concrete above the flexural crack before the yielding of the longitudinal reinforcement, which is called an overreinforced beam. These types of failures in a beam are called flexural failures [17].

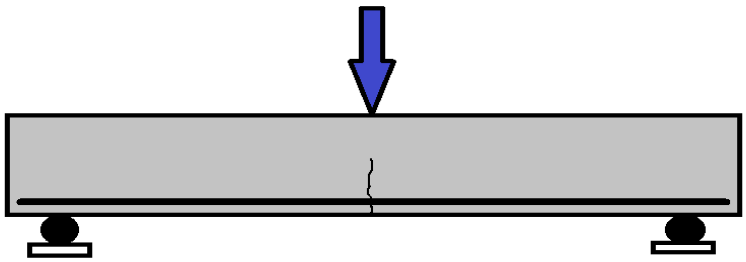

Fig. 1 Flexural failure.

4. Dimensions and details of specimens

Two specimens were used in our project.

1) Reinforced concrete beam with a cross section of (20 cm× 15 cm), and 102 cm length, four 10 mm longitudinal steel bars, and eight 6 mm stirrup steel bars were applied.

2) A reinforcement system was invented using a reinforced concrete beam with 4 mm × 10 mm longitudinal steel bars and 8 mm × 6 mm stirrup steel bars, and 16 steel plates with dimensions of 10 cm × 2.5 cm × 0.3 cm positioned starting from the stirrups in both the top and bottom zones and braced in two directions on the right and left sides across the beam length using 12-mm steel bars. A central bracing was placed at the center of the beam using 12-mm steel bars connected to both support plates at the bottom face of the concrete (see Figs. 2(a) and 2(b) below):

https://doi.org/10.1007/s11709-021-0706-z

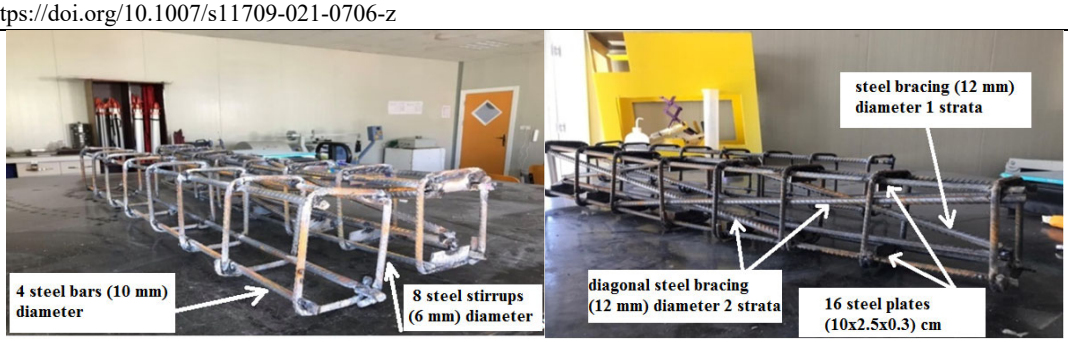

(a) (b)

Fig.2 Details of reinforcement. (a) Invented reinforcement; (b) ordinary reinforcement.

The details of the invented reinforcement system are shown in Figs. 3(a) and 3(b) below.

The aim of this reinforcement system is to add an auto stabilization of a high deflection at the center of the beam using the final result of both the compression and tension stresses through the use of bracings. This stabilization leads to higher compression and tensile strengths of the concrete, and a late yielding of the steel bars.

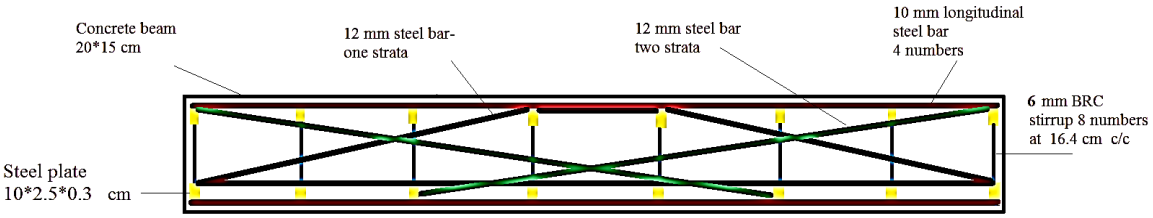

(a)

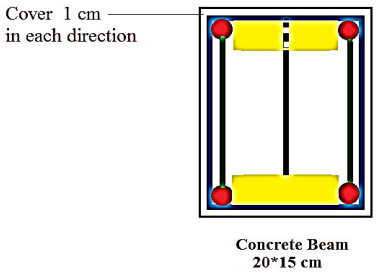

(b)

Fig. 3 Details of the invented reinforcement system. (a) Longitudinal section of the invented reinforcement; (b) Cross-section of the invented reinforcement.

5 Experiment results and discussion

The outputs of the three-point flexure test for the two specimens with loading rate of (0.1 MPa/s) are as follows.

1) An ordinary reinforced concrete beam specimen was fractured at a load of 46.54 kN with a duration of 348 s, which suffered from a high deflection. The compression face was cracked under the applied load (local compression failure), and the tension face showed wide local shear cracks.

2) The invented reinforced concrete beam specimen was fractured at a load of 54.72 kN with a duration of 64 s, and the deflection was extremely small compared to the previous specimen. The cracks, called inclined flexural-shear cracks, were extremely small, narrow, inclined, and straight in the middle span and along the beam (Fig. 4).

RESEARCH ARTICLE
https://doi.org/10.1007/s11709-021-0706-z

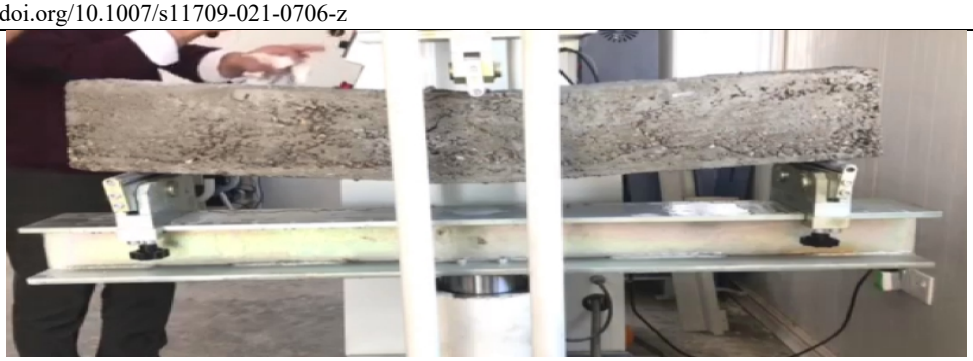

(a)

(b)

(c)

Fig. 4 Specimens after failure outside the instrument. (a) Ordinary specimen after failure; (b) invented specimen after failure; (c) failure of specimens outside the instrument.

The following Fig.5 shows load–deflection curves for both the ordinary reinforcement system and the invented reinforcement system. It is clear that the linear part of each case represents the elastic stage of each specimen under a load and the softening stage prior to failure. Both specimens can also be clearly seen to have two different points of failure. It is worth mentioning that for the ordinary reinforcement system, the maximum deflection is 4.641 cm, and for the invented reinforcement system, it is 1.563 cm.

RESEARCH ARTICLE
https://doi.org/10.1007/s11709-021-0706-z

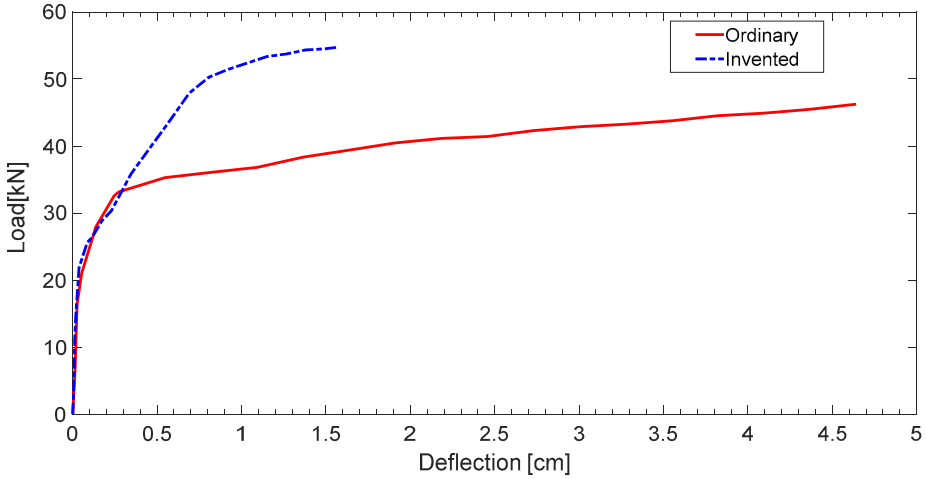

Fig. 5 Load-deflection curves.

The results in Table 1 indicate that the invented reinforcement system has a higher modulus of elasticity when bending, and thus withstands higher stresses and results in a lower strain. In addition, the invented specimen undergoes less maximum deflection reaching 1/3 of the maximum deflection for an ordinary specimen, which means that the stiffness increases for the invented reinforcement system. The flexural strength of the system also increased 15.5% in comparison with the ordinary reinforcement system, and the modulus of elasticity when bending was 14,224 MPa in comparison with the ordinary reinforcement system at 9345 MPa, which is an increase of 65.69%. Furthermore, the flexural strain used in the invented reinforcement system was 0.07, which compared with the same output in the ordinary reinforcement system at 0.024 is a decrease of 291.66%.

Table 1 Experimental results of the outputs for the specimens

specimen	E (MPa)	δ_{max} (mm)	σ (MPa)	ϵ (mm/mm)
ordinary	9345	46.41	10.288	0.070
invented	14224	15.63	12.175	0.024

6 Finite element models

Numerical simulations were calculated in LS-DYNA [18] using an explicated time integration scheme. Both models, with ordinary and invented reinforcement systems, were composed of three parts: concrete, a reinforcement, and the loading mechanism. The only difference between the models was the reinforcement.

Solid elements with a size of 5 mm were used to discretize the concrete block, with a total of 244800 elements. The ordinary reinforcement was simulated using only beam elements. The invented reinforcement system has additional shell elements to model the steel plates between the stirrups. The average size of the beam and shell elements was 10 mm. The connections between the rebars and stirrups and plates in the case of the invented reinforcement system were made using shared nodes. This means that the connection was modeled as a perfect weld connection. The connection between the concrete and reinforcement was applied using constraint-based coupling. Both accelerations and velocities were constrained to guarantee the appropriate force transfer between the concrete and reinforcement. The loading mechanism was modeled with rigid shell elements because the mechanism was not expected to undergo any deformation. The left and right supports were fixed, and the center cylinder with the prescribed vertical motion was fixed in the horizontal direction only. The interaction between the concrete and loading mechanism was achieved using a penalty-based contact with a segment detection of the contact penetration. With this approach, the contact penetration was limited during the loading, and the contact force oscillations were negligible. As previously mentioned, the loading was controlled through the prescribed displacement. The loading speed was constant as in the experiment; therefore, no strain rate effects were considered.

https://doi.org/10.1007/s11709-021-0706-z

The continuum surface cap model (CSCM) was used as a material model for concrete [19,20]. The CSCM implemented in LS-DYNA is extremely stable and is a good choice, particularly when not all mechanical properties of concrete are available, that is, measured. The CSCM in LS-DYNA can generate all required material parameters based on the given unconfined compressive strength (UCS). Of course, the user is allowed to overwrite the generated parameters if a better estimate of any parameter is available. The CSCM is based on the yield surface represented by following three stress invariants:

$$J_1 = 3P, \quad (7)$$

$$J_2' = \frac{1}{2} S_{ij} S_{ij}, \quad (8)$$

$$J_3' = \frac{1}{3} S_{ij} S_{jk} S_{ki}, \quad (9)$$

where J_1 is the first invariant of the stress tensor, J_2' is the second invariant the deviatoric stress tensor, and J_3' is the third invariant of the deviatoric stress tensor. The invariants are represented by the deviatoric stress tensor S_{ij} and pressure P [21]. The yield surface is defined as

$$f\left(J_1, J_2', J_3', \kappa\right) = J_2' - \Re^2 F_f^2 F_c, \quad (10)$$

where κ is the cap hardening parameter, F_f is the shear failure surface, F_C is the hardening cap, and $\Re$ is the Rubin three-invariant reduction factor. In addition, the parameters of the CSCM are listed in Table 2. The remaining CSCM parameters were internally generated based on the CEB-FIP data [21,22].

Table 2 Material parameters of the CSCM

parameter	value	unit
UCS, f_c	15.0	MPa
tensile strength, f_t	1.46	MPa
initial shear modulus, G_c	9.096	GPa
initial bulk modulus, K_c	9.962	GPa
maximum aggregate size, a_g	32	mm
fracture energy (uniaxial stress), G_{fc}	4213.0	$J \cdot m^{-2}$
fracture energy (uniaxial tension), G_{ft}	42.13	$J \cdot m^{-2}$
fracture energy (pure shear stress), G_{fs}	42.13	$J \cdot m^{-2}$

The material model of steel is a simplified elastic-plastic model with hardening. The initial Young's modulus of elasticity was 200 GPa and the tangential modulus was 2 GPa, which corresponds to 1% of the initial stiffness. The yield strength was estimated to be 220 MPa, as the steel quality was not the best. Both numerical models are shown in Fig. 6, where the center part of the concrete is hidden such that the reinforcement can be seen. The material parameters of steel are listed in Table 3, and were used for both reinforcement systems.

Table 3 Material parameters of steel

parameter	value	unit

https://doi.org/10.1007/s11709-021-0706-z

yield strength, f_y	220.0	MPa
elastic modulus, E_s	200.0	GPa
tangent modulus, E_{tan}	2.0	GPa
Poisson's ratio	0.3	–
ultimate strain, ε_{uk}	2.5	%

A mesh size sensitivity study was a part of the model preparation conducted at the beginning of the research. Because a softening of the concrete can lead to damage localization in the FE mesh, two element sizes of 5 and 10 mm were examined in detail. In this study, only the size of the concrete elements was changed. The results exhibited a small variation within 5% of the peak reaction force, with 10% of the initial stiffness; in addition, the fracture pattern was more or less identical, but was smeared in the case of the coarse mesh. However, there could be many reasons for this variation. Taking into account the contact formulation and the coupling algorithm, even more than a 10% variation is acceptable in most studies. Furthermore, the CSCM in LS-DYNA uses a regulation technique based on the constant energy of the fracture and the size of the element. From the given parameters and actual element size, the softening parameters are internally calculated and used. The CSCM regulation technique can be found in Refs. [21,22]. Because a concrete mesh size of 5 mm did not significantly increase the computational time, it was used in the simulations.

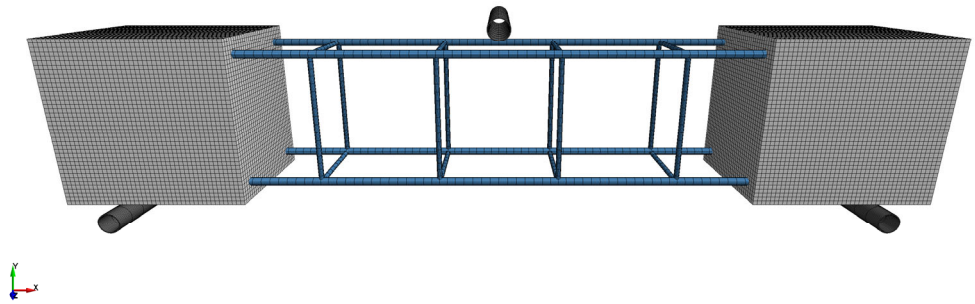

(a)

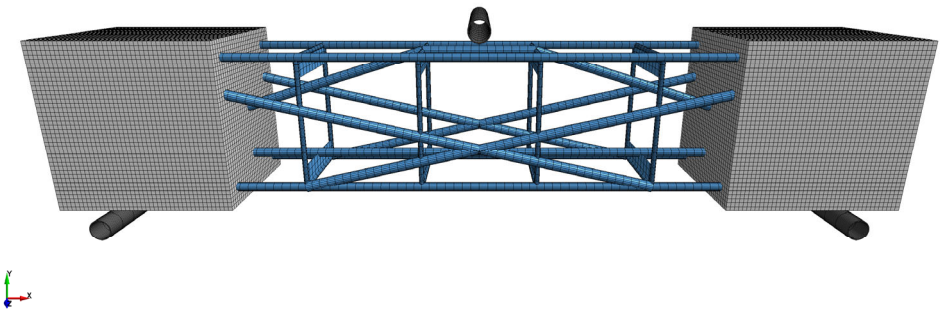

(b)

Fig.6 FE models of the RC beams. (a) Ordinary reinforcement system model; (b) invented reinforcement system model.

7 Verification of experimental results

The results of the four outputs from the simulations of both models (ordinary reinforcement system and invented reinforcement system) are shown in **Table 4**.

Table 4 Simulation results of the outputs for the models

specimen	E (MPa)	δ_{max} (mm)	σ (MPa)	ϵ (mm/mm)
ordinary	8710	46.397	10.261	0.070
invented	15140	14.133	12.183	0.021

7.1 Modulus of elasticity

From the simulation results with respect to the modulus of elasticity in terms of flexure (see Fig. 7), it can be seen that the ordinary model has a value of (8710 MPa) and the invented model is (15140 MPa), whereas if they are compared with the same results from the experimental tests (9345 MPa) and (14224 MPa), respectively, we can see that there is a difference of 6.8% for the ordinary reinforcement system, which is due to the non-homogenous material property of the ordinary experimental specimen and the ideal homogenous material property of the ordinary model in LS-DYNA, as well as an approximation of the calculated modulus of elasticity from the slope of the linear part of the load-deflection curve. Using the same approach as with the invented reinforcement system, we can see a difference of 6.1% for the same reason and a robust welding of the steel plates and stirrups on one side and between the steel plates and longitudinal reinforcement on the other side, whereas this firm connection cannot be modeled efficiently using LS-DYNA as it exists in the develop reinforcement system specimen.

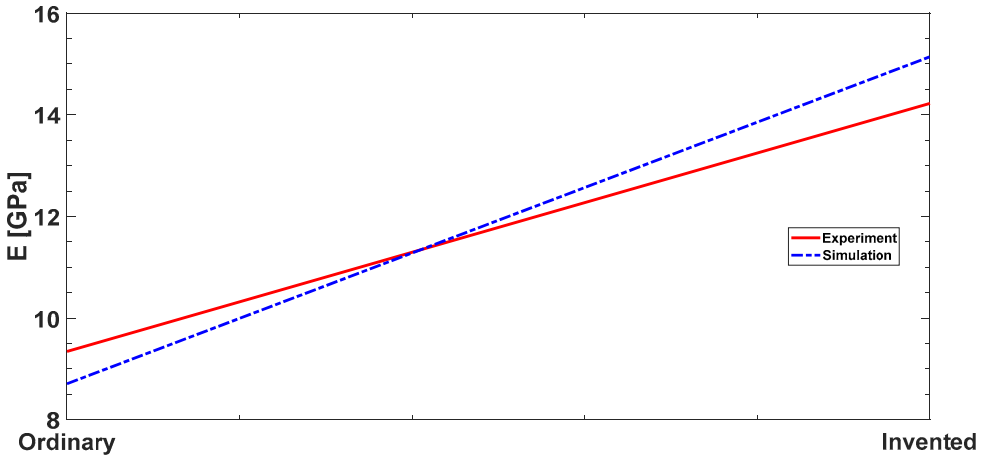

Fig. 7 Comparison-modulus of elasticity.

Furthermore, many points have effective roles in the different results obtained, e.g., a non-horizontal installment of the experimental machine, a rough surface of the concrete under the applied load, and non-ideal values of the elastic properties of the steel bars and steel plates for both ordinary and invented specimens, which have appreciable effects on the behavior of the structural member under the applied load.

7.2 Maximum deflection

This time, in the simulation results with respect to the maximum deflection (see Fig. 8), the ordinary model has a value of (46.397 mm) and the invented model is 14.133 mm. If they are compared with the same results from the experimental tests, which are 46.41 and 15.63 mm, respectively, we can see that the difference between the results for the maximum deflection output is 0.00028% for the ordinary reinforcement system model, which is an extremely efficient simulation of the actual behavior. For the invented reinforcement system model, the difference is 10%, which has a relatively large difference in representing the actual response of the invented RC beam under the applied load. We can relate the large difference to the same reasons mentioned for the modulus of elasticity output in the previous section, particularly the strong welding between

RESEARCH ARTICLE
https://doi.org/10.1007/s11709-021-0706-z

the reinforcement parts that cannot be modeled in the LS-DYNA as it exists in the experimental specimen.

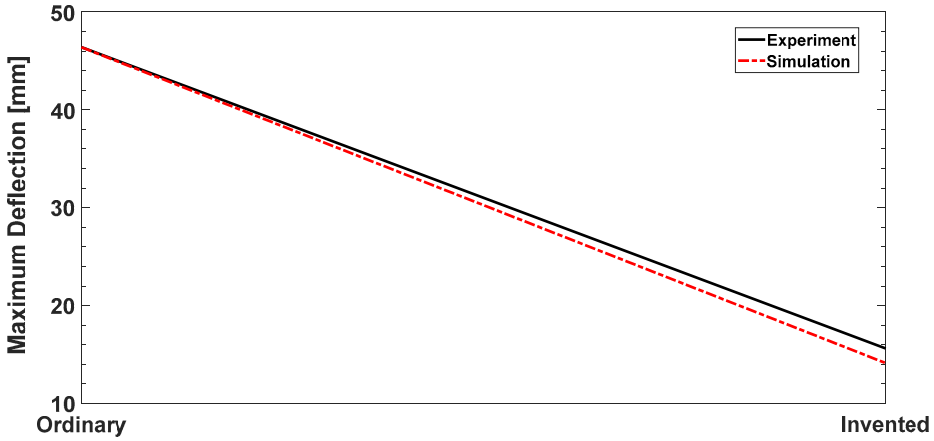

Fig. 8 Comparison of maximum deflection.

7.3 Flexural stress

The results of the simulations for the flexural stress (see Fig. 9) show that the ordinary model has a value of 10.261 MPa and the invented model is 12.183 MPa, and if they are compared with the same results from the experimental tests, which are 10.288 and 12.175 MPa, respectively, we can see that the difference between the results for the flexural stress output is 0.0026% for the ordinary reinforcement system model, which manifests an extremely efficient simulation of the actual behavior. By contrast, for the invented reinforcement system model, the difference is 1%, which is an extremely small difference in representing the actual response of the invented RC beam under the applied load. We can relate the efficient replication between the experimental and simulation outputs to a single issue, which is independent of the reasons mentioned above. This output can be calculated from a formula containing the applied force, effective beam span, and the cross-sectional dimensions of the beam.

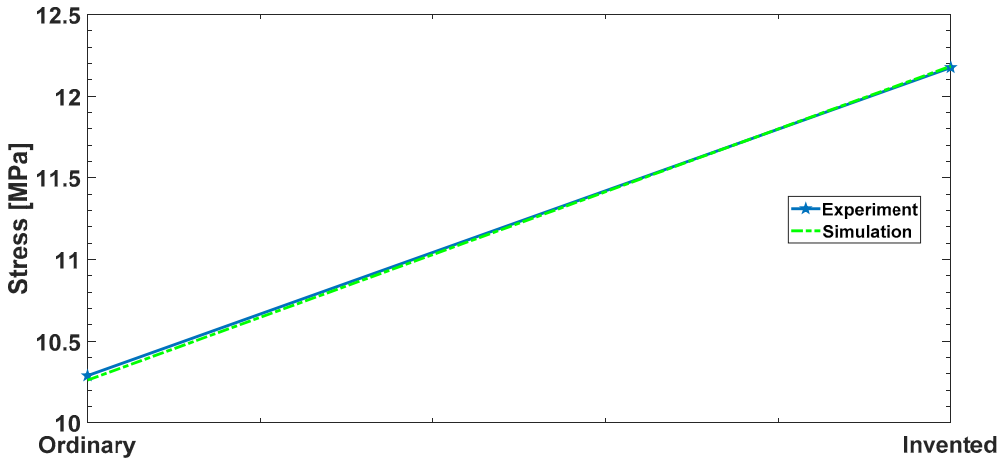

Fig. 9 Comparison-flexural stress.

7.4 Flexural strain

The results of the simulations for the flexural strain (see Fig. 10) show that the ordinary model has a value of 0.070 mm/mm, and the invented model is 0.021 mm/mm. If they are compared with the same results from the experimental tests, which are 0.070 and 0.024 mm/mm, respectively, we can see that the variation between the results for the flexural strain output is 0.0% for the ordinary

https://doi.org/10.1007/s11709-021-0706-z

reinforcement system model, which manifests an excellent and efficient simulation of the actual behavior. For the invented reinforcement system model, the difference is 12.5%, which has a wide difference in representing the actual response of the invented reinforced concrete beam under the applied load. We can explain the high difference between the two results for the invented reinforcement system for the same reasons mentioned for the modulus of elasticity output in the previous section, particularly the strong welding between the reinforcement parts that cannot be modeled in the LS-DYNA as it exists in the experimental specimen. The strong welding between the bracing parts in the experimental specimen for the invented reinforcement system results in a late yield of the steel and earlier yielding of the concrete material. As a result, much higher strains occur in the concrete for the specimen of the invented reinforcement system as compared with the same model used in the simulation.

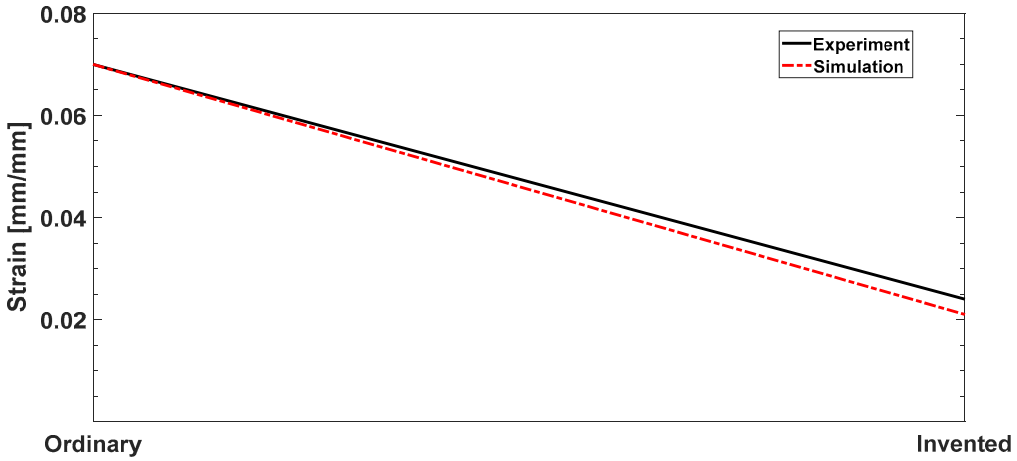

Fig. 10 Comparison of flexural strain.

7.5 Load-deflection curves

The load-deflection curves for both models, which were determined from the simulations, are highly similar to the load-deflection curves obtained from the experimental tests using the three-point bending machine (see Figs. 11 and 12), particularly at the beginning of the loading stage and the end of the softening stage for both of the specimens with little fluctuation at the beginning of the softening stage owing to the difference in elastic properties of both specimens as compared to the ideal elastic properties for the constructed models in the LS-DYNA, in addition to the geometrical differences between the experimental specimens and the numerical models. Furthermore, the differences in the method used to apply the load and the contact conditions between the applied load and the top surface of the specimen are compared with the models constructed during the simulations.

RESEARCH ARTICLE
https://doi.org/10.1007/s11709-021-0706-z

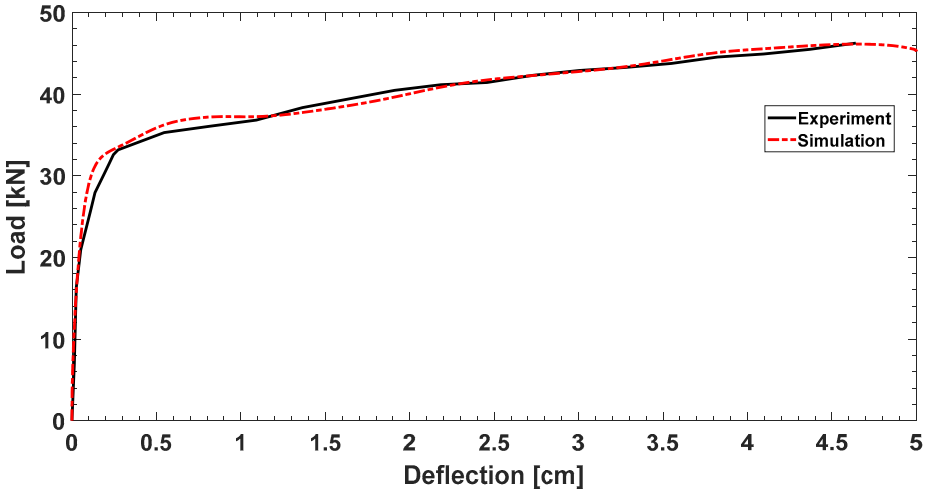

Fig. 11 Load-deflection curves in ordinary reinforcement system.

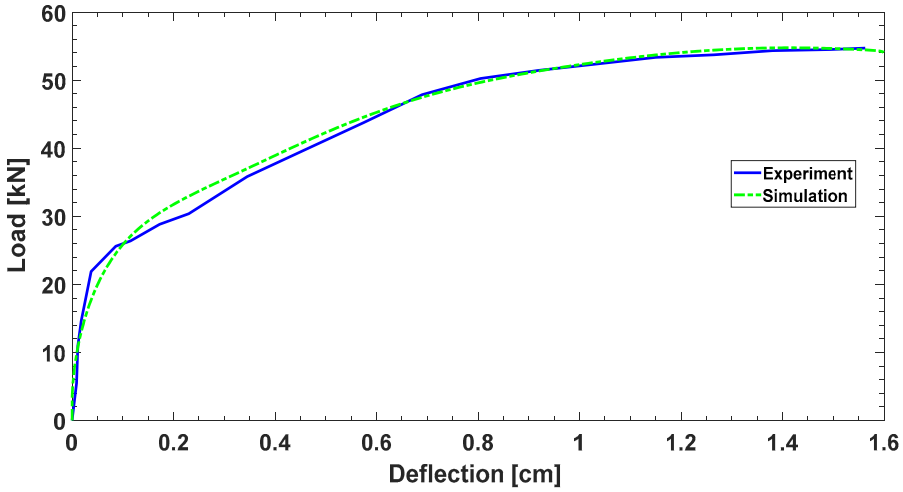

Fig. 12 Load-deflection curves in invented reinforcement system.

6 Flexural failure in ordinary specimen

The failure of the ordinary reinforcement system model when using the LS-DYNA simulation shows the same crack pattern when comparing with the failure of the specimen of the same model in the experimental test (see Fig. 13). The cracks are wide, starting under the applied load, and also propagate from the tension zone of the beam where the failure occurs owing to the yielding of the steel before the concrete fails. The large deflection in both numerical model and the experimental test is also another significant result of the comparison. The flexural stress at failure during the simulation was 10.261 MPa, and the flexural stress at failure for the experimental specimen was 10.288 MPa.

https://doi.org/10.1007/s11709-021-0706-z

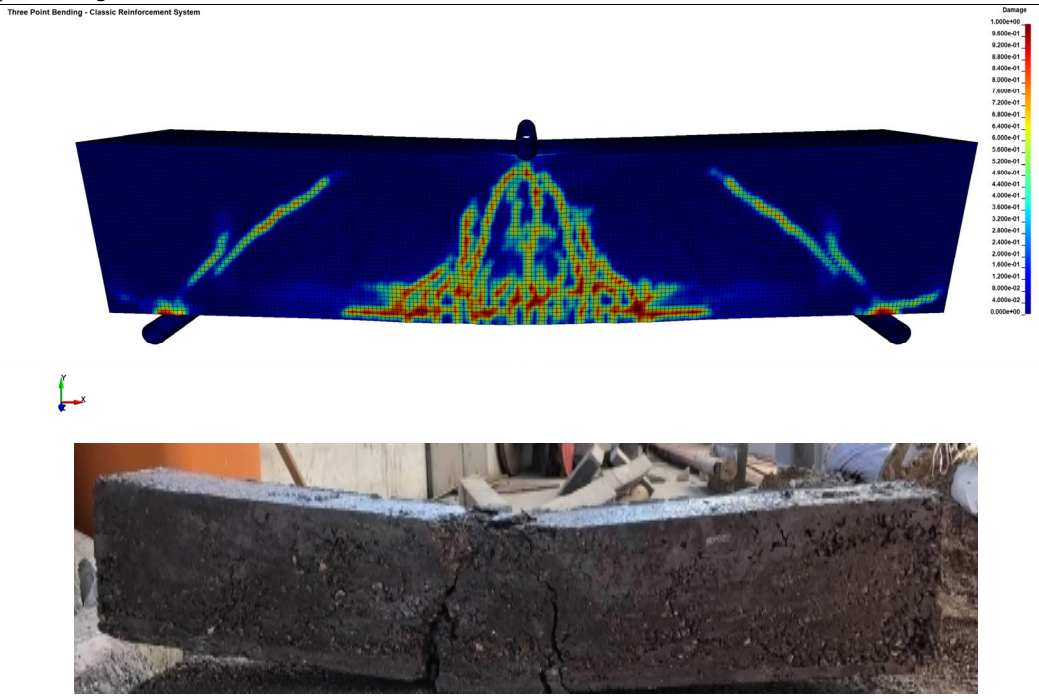

Fig. 13. Verification of the results for an ordinary reinforcement system.

7.7 Flexural failure in invented specimen

The failure of the invented reinforcement system model in LS-DYNA has the same crack pattern as in the experimental test. The cracks are narrow starting under the applied load and propagate from the tension face and spread along the effective span of the beam where the failure occurs owing to the concrete failure before the steel yields. We can see an extremely good replication between both the failure pattern and the applied flexural stress, both of which have an extremely small number of deflections owing to robust welding between the reinforcement system and the auto-stabilization mechanism by the support of the steel plates and the three additional bracing systems. The flexural stress at failure for the simulation was 12.183 MPa, and the flexural stress at failure for the experimental specimen was 12.175 MPa.

8 Conclusions

Experimental tests and a numerical analysis using the LS-DYNA program were conducted to study the flexural strength and stiffness of an invented reinforcement system for a concrete beam. The results of numerous outputs were calculated from both methods and compared to determine the success of the new reinforcement system. The following points can be made.

1) The invented reinforcement system increased the bending strength of the reinforced concrete beam to 15.5%.

2) The invented reinforcement system decreased the maximum deflection of the reinforced concrete beam to a ratio of 1/3. As a result, the stiffness of the RC beam was enhanced.

3) The adoption of the invented reinforcement system decreased the compression and tension damage to an excellent range, where only small microcracks were generated under higher flexural loading. Consequently, the behavior of the reinforced concrete beam has been modified from ductile to brittle owing to a higher ρ value and late yielding of steel.

4) The simulations manifested significant replications of the responses for both experimental specimens in relation with the stiffness and flexural failure patterns.

Acknowledgements This study was conducted with the financial support from the project GACR 17-23578S “Damage assessment identification for reinforced concrete subjected to extreme loading” provided by the Czech Science Foundation. Furthermore, we acknowledge the

cooperation of the civil engineering department of Tishk International University-Sulaimani in the Kurdistan Region of Iraq, who granted us official permission to conduct the experimental tests on the two specimens at their concrete laboratory.

References

1. Jusoh W A W, Ibrahim I S, Sam A M. Flexural behavior of reinforced concrete beams with discrete steel–polypropylene fibers. MATEC Web of Conferences, 2017, 101: 01020 doi:10.1051/matecconf/201710101020

2. Isa M N. Flexural improvement of plain concrete beams strengthened with high performance fiber reinforced concrete. Nigerian Journal of Technology, 2017, 36(3): 697–704

3. Adom-Asamoah M, Wiafe Ampofo J, Afrifa R O. Flexural and shear behavior of reinforced concrete beams made from recycled materials. Journal of Ghana Institution of Engineers, 2009, 6(1): 57–66

4. Rabczuk T, Bordas S, Zi G. On three-dimensional modelling of crack growth using partition of unity methods. Computers & Structures, 2010, 88(23–24): 1391–1411 doi:10.1016/j.compstruc.2008.08.010

5. Rabczuk T, Zi G, Bordas S, Nguyen-Xuan H. A simple and robust three-dimensional cracking-particle method without enrichment. Computer Methods in Applied Mechanics and Engineering, 2010, 199(37–40): 2437–2455 doi:10.1016/j.cma.2010.03.031

6. Rabczuk T, Belytschko T. A three dimensional large deformation meshfree method for arbitrary evolving cracks. Computer Methods in Applied Mechanics and Engineering, 2007, 196(29–30): 2777–2799 doi:10.1016/j.cma.2006.06.020

7. Rabczuk T, Belytschko T. Cracking particles: A simplified meshfree method for arbitrary evolving cracks. International Journal for Numerical Methods in Engineering, 2014, 61(13): 2316–2343

8. Rabczuk T, Zi G, Bordas S, Nguyen-Xuan H. A geometrically non-linear three dimensional cohesive crack method for reinforced concrete structures. Engineering Fracture Mechanics, 2008, 75(16): 4740–4758 doi:10.1016/j.engfracmech.2008.06.019

9. Shishegaran A, Ghasemi M R, Varaee H. Performance of a novel bent-up bars system not interacting with concrete. Frontiers of Structural and Civil Engineering, 2019, 13(6): 1301–1315 doi:10.1007/s11709-019-0552-4

10. Mohammad R G, Aydin S. Role of slanted reinforcement on bending capacity SS beams. Vibroengineering procedia, 2017, 11: 195–199 doi:10.21595/vp.2017.18544

[**11**] Namdar A, Darvishi E, Feng X. Effect of Flexural crack on plain concrete beam failure mechanism a numerical simulation. Fracture and Structural Integrity, 2016, 36: 168-181

12. Masmoudi A, Ben Ouezdou M, Haddar M. Mode of failure for reinforced concrete beams with GFRP bars. Journal of Theoretical and Applied Mechanics, 2016, 54(4): 1137–1146 doi:10.15632/jtam-pl.54.4.1137

13. Lana D d S G, Denio R. C d O, Bernardo N d M N, Adelson B d M, Alcebiades N M, Francisco A C d S. Experimental analysis of the efficiency of steel fibers on shear strength of beams. Latin American Journal of Solids and Structures, 2018, 15(7): 1–16

14. Sudarsana K, Sajana P C, Gusti N O S. Applications of bolted steel plates to shear strengthening of RC beams. MATEC Web of Conferences, 2019, 276: 01002

[**15**] Chen W F. Elasticity and Plasticity. Beijing: Chinese Architecture and Building Press, 2003

16. Perez N. Fracture Mechanics. Amsterdam: Kluwer Academic Publishers, 2004

17. Ziara M M. The Influence of Confining the Compression Zone in the Design of Structural Concrete Beams. Edinburgh: Heriot-Watt University, 1993

18. Livermore Software Technology Corporation. LS-DYNA Theory Manual. Livermore, CA: LSTC, 2020

19. Muttoni A. Punching shear strength of reinforced concrete slabs without transverse reinforcement. ACI Structural Journal, 2008, 105: 440–450

20. Mutton A, Ruiz M F. Shear strength of members without transverse reinforcement as function of critical shear crack width. ACI Structural Journal, 2008, 105: 163–172

21. Murray Y D. User's Manual for LS-DYNA Concrete Material Model 159. FHWA-HRT-05-062. 2007

[**22**] Murray Y D, Abu-Odeh A, Bligh R. Evaluation of Concrete Material Model 159. FHWA-HRT-05-063. 2007